Fast and Slow Dynamics of Isotactic Polypropylene Melts

Jeerachada Tanchawanich and Valeria Arrighi*

Chemistry, School of Engineering and Physical Science, Heriot-Watt University, Edinburgh EH14 4AS, UK

Maria Carmela Sacchi

Istituto per lo Studio delle Macromolecole, ISMAC-C.N.R, Milano, Italy

Mark T. F. Telling

ISIS, Rutherford Appleton Laboratory, Chilton, Didcot OX11 OQX, UK

Alessandro Triolo

Istituto Processi Chimico-Fisici, Sezione di Messina-CNR, Messina, Italy

Received June 26, 2007; Revised Manuscript Received December 20, 2007

ABSTRACT: We report a quasi-elastic neutron scattering (QENS) study of local dynamics in isotactic polypropylene (iPP) melts. QENS measurements were carried out on the spectrometer IRIS (ISIS, UK), using a series of selectively deuterated iPP samples. Analysis of the intermediate incoherent scattering functions was conducted using two different models: (a) a two-component model involving a fast process and conformational transitions and (b) a three-component model including methyl group reorientations. We show that consistent results between the selectively deuterated samples are only obtained when methyl group reorientations are explicitly taken into account. The results presented here are consistent with the simulated intermediate scattering functions of atactic polypropylene [Ahumada, O.; Theodorou, D. N.; Triolo, A.; Arrighi, V.; Karatasos, C.; Ryckaert, J.-P. *Macromolecules* **2002**, *35*, 7110] which revealed contributions from torsional transitions of the methyl groups and segmental motion, in addition to a fast process.

Introduction

Polypropylene is a vinyl polymer that can be synthesized in different tactic forms. The fully amorphous atactic isomer (aPP) has been extensively investigated, and several dynamic studies reported in the literature have dealt with motion at either microscopic[1−9] or macroscopic length scales.[10−20] Fewer dynamic investigations have been carried out on isotactic (iPP) and syndiotactic polypropylenes (sPP), but it is known that stereoregularity has a pronounced effect on polymer properties; notably, it leads to formation of highly crystalline structures from the regular isotactic and syndiotactic stereoisomers while atactic polymers are amorphous. Experiments carried out on polypropylenes have shown that tacticity affects polymer structure, conformation, and packing.[21] Furthermore, NMR[4,7,22,23] and rheological[18] measurements indicate that stereoregularity plays an important role in melt dynamics and viscoelastic properties. Computer simulation studies have been instrumental in understanding local PP dynamics in the melt state[24,25] and solution.[26]

In a previous publication,[8] we reported analysis of quasi-elastic neutron scattering (QENS) data of the three PP stereoisomers. Compared to other experimental methods, the technique of quasi-elastic neutron scattering which is also employed here affords dynamic information on a local scale, up to a few monomer units, and at high frequency. It is therefore suitable to investigate segmental motion, side-group rotations, and faster processes. In this paper we examine in more detail the local motion of isotactic polypropylene melts and, using selectively deuterated samples, aim to separate the different contributions to the observed dynamics.

In our previous study,[8] qualitative comparison between the elastic neutron scattering intensities of aPP, iPP, and sPP, as a function of temperature, showed that stereoregularity has little if any effect on sub-T_g dynamics. Unlike other polymers, e.g., poly(methyl methacrylate),[27] the activation energy associated with methyl group rotations, and its distribution, are very similar for the three PP stereoisomers.

In the melt state, several molecular processes contribute to the observed dynamics. It is suggested by MD simulations[2] that the dynamic incoherent structure factor measured by neutron scattering above the glass transition, T_g, should reveal four distinct processes: (1) localized motions, i.e., the librations of the methyl groups around their stems, bond angle bending vibrations, and torsional oscillations of the backbone bonds, (2) torsional jumps of methyl groups, (3) segmental motion associated with conformational transition, and (4) the diffusional motion of short chains, which can only be detected at significantly small Qs. However, one usually invokes a simpler model to describe the QENS data and in doing so accounts for contributions from only fast and slow processes. This procedure has been adopted by us in the description of the intermediate scattering function of PP.[2,8,28] It is based on the assumption that all protons are to be treated equally, and no attempts are made to separate contributions from methyl group and segmental motion above T_g, except in a few cases (see, for example, ref 29). However, the incoherent dynamic structure factors computed from MD simulations on different polymeric systems suggest that a more appropriate procedure should account for the influence of side-group motions, for example methyl group

* Corresponding author: Fax +44 (0) 131 451 3180; Ph +44 (0) 131 451 3180, e-mail v.arrighi@hw.ac.uk.

10.1021/ma071412w CCC: $40.75
Published on Web 02/05/2008

Table 1. Glass Transition and Melting Temperatures of PP Samples Investigated in This Work

label	repeat unit	T_g (K)	T_m (K)
iPP-H	$-CH_2-CH(CH_3)-$	260	435
iPP-D1	$-CH_2-CD(CH_3)-$	264	438
iPP-D2	$-CHD-CD(CH_3)-$	268	430
iPP-D5	$-CHD-CD(CD_3)-$	267	395

dynamics in polyisoprene melts.[30] In this respect MD simulations suggest that the methyl group relaxation and the segmental motion should be resolved in time scale,[2] but there seems to be no apparent separation of these two processes in experimental data.[8,28] In order to clarify this point, QENS experiments were carried out on selectively deuterated and hydrogenated PP samples, and a model that accounts for CH_3 contributions was used to analyze the QENS spectra.

Experimental Section

Materials. The selectively deuterated monomers were prepared as described in previous papers.[31−34] The isotactic polypropene samples were obtained in the presence of the $TiCl_3HRA-Al(C_2H5)_2I$ catalyst system in *n*-heptane at 30 °C. The monomer structures of the selectively deuterated materials are given in Table 1.

Isotactic polypropylene (iPP-H) was purchased from Aldrich. The sample had a weight-average molar mass of 12 000 g mol^{-1}.

Differential Scanning Calorimetry. Glass transitions (T_g) and melting temperatures (T_m) were determined using a TA Instruments DSC 2010 with both heat flow and temperature scales calibrated against indium metal. Nitrogen was used as purge gas, and samples were scanned at 20 °C min^{-1}. The glass transition, T_g, and melting temperature, T_m, of the partially deuterated iPP samples are listed in Table 1, together with the structure of the polymer repeat unit. All T_g values in Table 1 refer to the midpoints of the inflections.

Neutron Scattering Measurements. QENS measurements were carried out on the high-resolution backscattering spectrometer IRIS (ISIS, Rutherford Appleton Laboratory, UK) in the temperature range 440−500 K.[35] QENS data were collected using the PG002 analyzers, giving energy resolution of 15 μeV. The energy range covered in this experiment varied from −0.2 to 1.2 meV, with a Q range from 0.5 to 1.8 $Å^{-1}$.

A slab cell was used in all measurements giving sample thicknesses of ca. 0.2 mm. This is equivalent to a transmission of ca. 0.9, and it ensures that multiple scattering effects are kept to a minimum and can be neglected in the analysis.

The dynamic incoherent structure factor, $S(Q,\omega)$, was computed from the time-of-flight data, after subtracting the contribution of the empty cell and correcting for absorption, using standard software, available at ISIS.[36] The dynamic structure factor, $S(Q,\omega)$, was transformed into the time domain intermediate scattering function, $I(Q,t)$, by Fourier transform.[37]

Results and Discussion

Measurements of the neutron scattered intensity as a function of both energy and momentum transfer, Q ($Q = (4\pi/\lambda)\sin(\theta/2)$, where λ is the neutron wavelength and θ is the scattering angle), provide detailed dynamic information through analysis of the incoherent dynamic structure factor.[38] The double differential scattering cross section, $\partial^2\sigma/(\partial E\ \partial\Omega)$, which is experimentally measured, defines the probability that a neutron is scattered with energy change ΔE into the solid angle $\Delta\Omega$. While the cross section σ may include both coherent and incoherent contributions, for polymeric systems, motion is mainly detected through the incoherent scattering of the hydrogen atoms, since the incoherent cross section of hydrogen is much larger than the coherent and incoherent cross sections of the other atoms in the monomer units (C,O, etc.). Furthermore, the incoherent cross section of hydrogen (82.02 barns) is much larger than that of deuterium (2.05 barns), and therefore use of selectively deuterated samples coupled with neutron scattering measurements affords separation of molecular motions.

In order to extract dynamic information from the measured incoherent structure factors, it is necessary to select an appropriate model function for the incoherent scattering law, $S_{inc}(Q,\omega)$, which provides an expression in terms of molecular parameters. This function is then convoluted with the instrumental resolution and fitted to the experimental data.

In this paper as well as some of our previous publications,[8,28] we analyze the intermediate scattering function, $I_{inc}(Q,t)$, obtained by Fourier transform of the experimental data and after dividing by the Fourier transform of the resolution function. The relationship between $S_{inc}(Q,\omega)$ and the intermediate scattering function is

$$S_{inc}(Q,\omega) = \frac{1}{2\pi}\int I_{inc}(Q,t)\exp(-i\omega t)\,dt \qquad (1)$$

with

$$I_{inc}(Q,t) = \frac{1}{N}\sum \langle \exp(iQR_i(t))\exp(-iQR_i(0))\rangle \qquad (2)$$

where the brackets indicate thermal averaging and $R_i(t)$ and $R_i(0)$ are the position of the nuclei at time t and $t = 0$, respectively. As shown by eqs 1 and 2, $S_{inc}(Q,\omega)$ and $I_{inc}(Q,t)$ define the positions of the scattering nuclei within a sample as a function of time, and as such they convey dynamic information on the system.

Depending on temperature and experimental energy range, the measured intermediate scattering function may need to be expressed as the product of different dynamic contributions, e.g., vibrations, rotations, and translations of the scattering centers. (This is true if the assumption of dynamically decoupled molecular motion holds.) In our previous study,[8] analysis of the intermediate scattering function of polypropylene melts was carried out considering two contributions

$$I_{inc}(Q,t) = I^{lib}(Q,t)I^{seg}(Q,t) \qquad (3)$$

$I^{lib}(Q,t)$ representing fast librations on the picosecond time scale and $I^{seg}(Q,t)$ related to the slower segmental motion. The former was described by an exponential decay while the latter was identified with a stretched exponential function. Thus, the intermediate scattering function is given by

$$I(Q,t) = \left[A_f(Q) + (1 - A_f(Q))\exp\left(-\frac{t}{\tau_{fast}}\right)\right]\exp\left(-\frac{t}{\tau_{KWW}}\right)^{\beta} \qquad (4)$$

where τ_{fast} and $A_f(Q)$ are the characteristic time and the Q and temperature dependent amplitude of the fast process, respectively.

As described elsewhere,[8] analysis of the $I(Q,t)$ data of iPP-H using eq 4 was carried out by assuming β to be a Q independent parameter, while the Q dependence of τ_{KWW} was considered to follow a power law expressed as $\tau = \tau_0 Q^{-n}$, where τ_0 corresponds to the relaxation time at $Q = 1$ $Å^{-1}$. Moreover, a further assumption was made that τ_{fast} is equal to 0.5 ps, a value in close agreement with ^{13}C NMR[3,6,7] measurements, MD simulations,[2] and several reports on other polymeric systems (for example, refs 39 and 40).

The resulting fitting parameters are $\beta = 0.53 \pm 0.1$, $\tau_0 = 9.12 \pm 0.38$ ps, and $n = 2.8 \pm 0.4$, as reported in ref 8. Values of $A_f(Q)$ show the expected Q^2 dependence, a feature of the

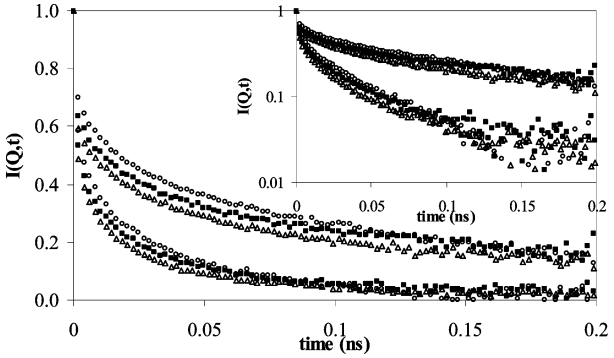

Figure 1. Intermediate scattering function of iPP-D5 (empty circles), iPP-D2 (filled squares), and iPP-D1 (empty triangles) at 440 K and two different Q values (0.55 and 0.95 Å^{-1} in order of decreasing intensity). Inset shows the same data in semilogarithmic scale.

Table 2. Fitting Parameters Derived from Fits of the $I(Q,t)$ Data Using Eq 4

sample	temp (K)	β	τ_0 (ps)	n	χ^2
iPP-D1	440	0.50 ± 0.03	12.31 ± 0.11	2.9 ± 0.1	5.87×10^{-2}
iPP-D2	440	0.52 ± 0.04	16.04 ± 0.17	3.0 ± 0.1	1.14×10^{-1}
	460	0.50 ± 0.04	9.89 ± 0.13	3.1 ± 0.1	1.14×10^{-1}
iPP-D5	440	0.67 ± 0.06	23.52 ± 0.25	2.6 ± 0.1	2.23×10^{-1}
iPP-H	460	0.51 ± 0.02	8.10 ± 0.07	3.1 ± 0.1	3.90×10^{-2}
	480	0.48 ± 0.03	5.43 ± 0.06	3.1 ± 0.1	4.32×10^{-2}
	500	0.50 ± 0.04	4.15 ± 0.06	3.1 ± 0.1	6.24×10^{-2}

Lamb−Mossbauer factor (LMF). However, as noted by us before,[8] $A_f(Q)$ shows little, if any, temperature dependence within the present experimental range.

The $I(Q,t)$ data of the selectively deuterated iPP samples at 440 K are compared in Figure 1. The $I(Q,t)$ curves of iPP-D5, which has negligible contributions from methyl group rotations, decay at a slower rate than those of iPP-D2, which contains contributions from both backbone and methyl group protons. These two samples have very similar glass transitions (Table 1), and therefore differences in their dynamic behavior should be a result of differences in proton dynamics.

Direct comparison between $I(Q,t)$ data of iPP-D1 and iPP-D2, which differ in the number of backbone protons in the repeat unit, cannot be made because of differences between the samples' T_g (Table 1). The lower T_g of iPP-D1 causes a faster relaxation for this polymer compared to iPP-D2, as observed in the experimental data of Figure 1.

The decay curves were fitted using eq 4 with the assumption that τ_{fast} is constant with Q and temperature and that $A_f(Q)$ is temperature independent. Fit results are reported in Table 2, and examples of fits are shown in Figure 2 for iPP-D2. It is noteworthy that the β parameters of iPP-D1, i-PP-D2, and iPP-H are almost identical, within experimental error. However, there is a large discrepancy between the average β value among these samples and that of iPP-D5 (0.67 ± 0.06). Comparison between τ_0 values of iPP-D2 and iPP-D5 shows that the relaxation time of iPP-D2 ($\tau_0 = 16.04 \pm 0.17$ ps at 440 K) is smaller compared to that of iPP-D5 ($\tau_0 = 23.52 \pm 0.25$ ps at 440 K), once again suggesting faster relaxation for the former sample compared to the latter. Furthermore, the Q dependence is more pronounced for iPP-D2 ($n = 3.0 \pm 0.1$) than for iPP-D5 ($n = 2.6 \pm 0.1$).

The differences in dynamic behavior of the selectively deuterated samples mentioned above suggest that motion of methyl groups takes place within the experimental time scale. On the basis of MD simulations,[2] rotation of methyl groups should be faster than the segmental process, resulting in the faster decay observed for iPP-D2. In addition, the broader distribution observed for iPP-D2 could be explained by considering that when fitting data using eq 4 a single KWW function is used to describe two elementary dynamic processes having different characteristic times. Thus, on the basis of numbers of protons in the backbone per repeating unit, one should expect the dynamics of iPP-H to be slower than that of iPP-D2, with iPP-D1 exhibiting intermediate behavior. Also, the relaxation time of iPP-D5 is expected to be highest among these samples, as there is no dynamic contribution from the methyl groups.

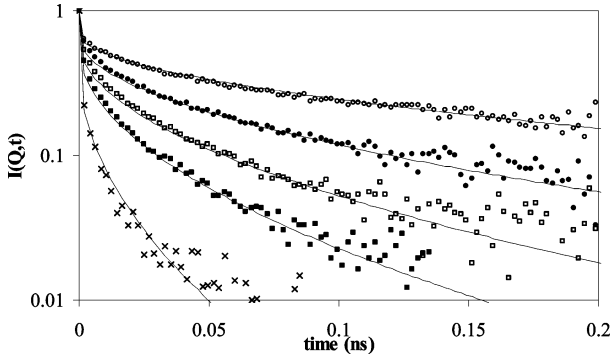

Figure 2. Intermediate scattering function of iPP-D2 at 440 K. The different curves refer to the following Q values: 0.55, 0.76, 0.95, 1.13, and 1.58 Å^{-1}, in decreasing order. Lines correspond to fits using eq 4.

We therefore conclude that, as also suggested by MD,[2] the contribution of methyl group rotational motion is far from negligible, in the temperature range 400−480 K. Hence, a more appropriate model that would consistently describe the $I(Q,t)$ data of the selectively deuterated i-PP samples should account for contributions from the fast process, methyl group rotation, and segmental motion. This translates in an intermediate scattering function of the form

$$I(Q,t) = I^{fast}(Q,t)\, I^{CH_3}(Q,t)\, I^{seg}(Q,t) \tag{5}$$

which is expressed as the product of fast, $I^{fast}(Q,t)$, methyl group, $I^{CH_3}(Q,t)$, and segmental, $I^{seg}(Q,t)$, dynamical processes.

By expressing the fast process, methyl group rotation, and segmental relaxation in terms of an exponential decay, a log−Gaussian distribution of exponential functions, and a KWW function, respectively, the $I(Q,t)$ can be written as

$$I(Q,t) = \left[A_f(Q) + (1 - A_f(Q)) \exp\left(-\frac{t}{\tau_{fast}}\right)\right] \times \left[A_0'(Q) + (1 - A_0'(Q)) \sum_{i=1}^{N} g_i \exp\left(-\frac{t}{\tau_i}\right)\right] \exp\left(-\frac{t}{\tau_{KWW}}\right)^{\beta} \tag{6}$$

where the weight factors, g_i, corresponding to the characteristic time, τ_i, are computed using a log−Gaussian distribution with the most probable characteristic time, τ_o. The parameter $A_0'(Q)$ is related to the elastic incoherent structure factor $A_0(Q)$, and it accounts for the fraction of immobile backbone protons through the relationship

$$A_0'(Q) = \frac{p_f}{p_{tot}} + \frac{p_m}{p_{tot}} A_0(Q) \tag{7}$$

where p_f, p_m, and p_{tot} represent the fraction of fixed, mobile, and total protons, respectively.

$A_0(Q)$ is the elastic incoherent structure factor (EISF) which represents the space-Fourier transform of the final distribution of the scatterers averaged over all possible initial positions. This

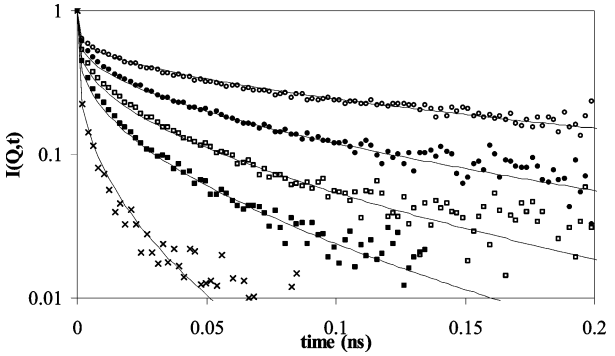

Figure 3. Intermediate scattering function of iPP-D2 at 440 K. The different curves refer to the following Q values: 0.55, 0.76, 0.95, 1.13, and 1.58 Å^{-1}, in decreasing order. Lines correspond to fits obtained using eq 6, consisting of three contributions (fast process, methyl group rotation, and segmental motion).

Table 3. Parameters and Goodness of Fit Obtained by Fitting $I(Q,t)$ Data Using a Model Consisting of Three Contributions: Fast Process, Methyl Group Rotation, and Segmental Motion (Eq 6)

sample	temp (K)	β	τ_0 (ps)	n	χ^2
iPP-D1	440	0.53 ± 0.03	16.28 ± 0.15	2.6 ± 0.1	5.96×10^{-2}
iPP-D2	440	0.58 ± 0.04	23.15 ± 0.27	2.6 ± 0.1	1.14×10^{-1}
	460	0.54 ± 0.05	14.09 ± 0.19	2.8 ± 0.1	1.16×10^{-1}
iPP-D5	440	0.67 ± 0.06	23.52 ± 0.25	2.6 ± 0.1	2.23×10^{-1}
iPP-H	460	0.54 ± 0.03	10.39 ± 0.09	2.9 ± 0.1	3.94×10^{-2}
	480	0.51 ± 0.03	6.95 ± 0.07	2.9 ± 0.1	4.39×10^{-2}
	500	0.52 ± 0.04	5.23 ± 0.07	2.9 ± 0.1	6.23×10^{-2}

quantity which gives geometrical information on the molecular motion is, for a 3-fold rotation, expressed by

$$A_0(Q) = \frac{1}{3}[1 + 2j_0(Qr_{H-H})] \tag{8}$$

where j_0 is the zeroth-order Bessel function and r_{H-H} is the distance between the equilibrium sites of the hydrogen atoms.

To carry out fits using eq 6 and minimize the number of fitting parameters, several assumptions were made. First of all, to simplify the description of the fast process, τ_{fast} was kept constant to 0.5. $A_f(Q)$ values were obtained from fits of the overlapped $I(Q,t)$ curves. This procedure is more reliable than simply using adjustable $A_f(Q)$ and τ_{fast} since the experimental data are not very sensitive to the fast process.

Similarly to our work on poly(dimethylsiloxane) (PDMS),[29] the methyl group parameters were fixed to values obtained from low-temperature QENS measurements. Hence we used a jump frequency, Γ_∞, equal to 28.8 meV, obtained from inelastic incoherent neutron scattering measurements,[41,42] and a value of activation energy, $E_a \pm \sigma_E$, equal to 14.5 ± 3.5 kJ/mol.[2,8,28] Therefore, only β, τ_0, and n were treated as fitting parameters.

The model appears to describe well the experimental data of all iPP samples, as shown by the examples of fits given in Figure 3 for iPP-D2. Fitting parameters and goodness of fits are reported in Table 3.

As discussed before, only fitting parameters obtained for iPP-D2 and iPP-D5 at 440 K are directly comparable because these two polymers have very similar glass transitions. As shown in Table 3, all β, τ_0, and n values relative to the slow process are now, within experimental error, very close, and this is contrary to the situation described earlier when using a model function consisting of only two components (eq 4).

In order to compare data reported in Table 3 with the results described earlier for the hydrogenated iPP sample, we need to account for differences between sample's T_gs. We have already

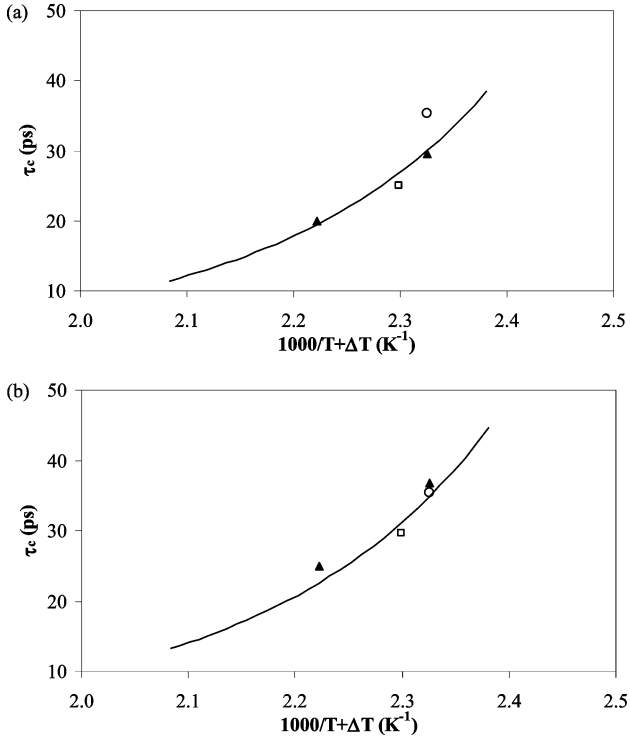

Figure 4. Correlation times of iPP-H (continuous line), iPP-D1 (empty square), iPP-D2 (filled triangles), and iPP-D5 (empty circle) obtained using (a) a model function consisting of two contributions (fast and slow processes; eq 4) and (b) a model function consisting of three contributions (fast process, methyl group rotation, and segmental motion; eq 6). The temperature axis has been shifted by ΔT (see the text) to account for differences in sample's T_g.

shown that the temperature dependence of the correlation time for PP stereoisomers above the glass transition follows the Vogel−Fulcher−Tamman (VFT) equation:[8]

$$\log \alpha_T = \log \frac{\tau(T)}{\tau_\infty} = \frac{B}{T - T_\infty} \tag{9}$$

By fitting the $I(Q,t)$ data of iPP-H using eq 6 at the different temperatures and after determining the correlation times

$$\tau_c = \tau_0 \frac{\Gamma\left(\frac{1}{\beta}\right)}{\beta} \tag{10}$$

the following VFT parameters for the slow process were obtained: $B = 528$, $T_\infty = 203$, and $\log \tau_\infty = -12.79$. These differ slightly from those reported previously,[8] based on fits using eq 4: $B = 554$, $T_\infty = 186$, and $\log \tau_\infty = -12.7$. (The τ_c values were calculated using an average $\beta = 0.52 + 0.02$.)

Figure 4a shows a comparison between correlation times determined from fits using eq 4. Data have been plotted vs $1/(T + \Delta T)$, where $\Delta T = T_{ref} - T_g$, i.e., the difference between a reference temperature T_{ref}, corresponding to T_g of iPP-H and the glass transition of the sample, T_g. While the correlation times of iPP-H, iPP-D2, and iPP-D1 are similar, iPP-D5 shows apparently slower dynamics.

The difference between correlation times is no longer evident in Figure 4b, where now data evaluated from fits using eq 6 are plotted. In particular, the correlation time of iPP-D5 is now close to the VFT curve determined for iPP-H. This suggests that the dynamic differences observed previously for the different samples are either to be related to the different glass

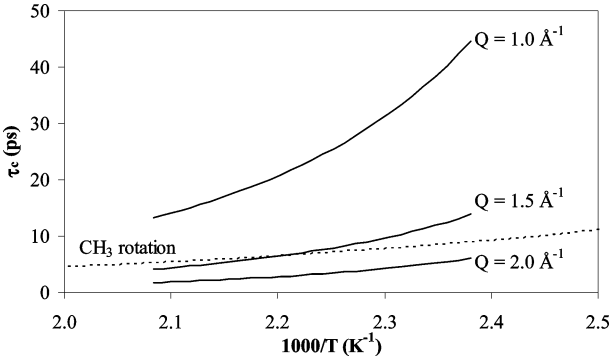

Figure 5. Relaxation map of iPP showing the temperature dependence of methyl group rotations (dashed line) and segmental process (full line) at different Q values (as indicated).

transitions or can be accounted for by the dynamic contribution from methyl group rotations. This suggests that the methyl group rotational motion takes place within the experimental range, and it can be described by the same unique set of parameters, Γ_∞, E_a, and σ_E found by modeling the QENS data at $T < T_g$.

One should note that the quality of the fits, as defined in terms of the summation of the residual error (see Tables 2 and 3), does not allow discriminating between the two models (eqs 4 and 6). Both appear to provide adequate description of the $I(Q,t)$ data at these temperatures and length scales. In addition, the similarity between the temperature dependence of the correlation time extracted from the two models that include or not contributions from methyl group rotations (eqs 4 and 6, respectively) indicates that the latter do not affect the temperature dependence of the relaxation time in the investigated Q and temperature ranges. Figure 5 shows the temperature dependence of the characteristic time for the methyl group and segmental processes, supporting these conclusions. It is found that at high Q, where the contribution from CH_3 rotations is more pronounced, the characteristic times of the segmental motion and methyl group rotation seem to overlap, while at low Q, where the difference between characteristic times is significant, the contribution from methyl group motion becomes trivial.

Conclusions

Quasi-elastic neutron scattering measurements on a series of selectively deuterated polypropylene samples were carried out and the intermediate incoherent scattering functions analyzed. Molecular dynamics simulations performed using a fully atomistic model on atactic polypropylene in the temperature range 260−600 K[2] had revealed three main regimes: (a) a rapid exponential decay which is attributed to fast motions, e.g., bond angle vibrations and torsional librations, (b) an intermediate regime associated with CH_3 reorientations, and (c) a slower nonexponential dynamics due to conformational transitions. While the contribution from torsional transitions of the methyl groups was clearly evident in the simulated $I(Q,t)$ decays arising from the methyl hydrogens,[2] this was not the case for the experimental $I(Q,t)$ data. Consequently, in our previous paper,[8] we considered a two-component dynamics which included only the fast process and segmental motion.

In this work, making use of selectively deuterated polypropylene samples, we show that it is possible to separate torsional jumps of the methyl groups and conformational transitions.

Acknowledgment. J.T. gratefully acknowledges financial support from Heriot-Watt University. The authors thank ISIS for beam time.

References and Notes

(1) Arrighi, V.; Pappas, C.; Triolo, A.; Pouget, S. *Physica B* **2001**, *301*, 157.
(2) Ahumada, O.; Theodorou, D. N.; Triolo, A.; Arrighi, V.; Karatasos, C.; Ryckaert, J.-P. *Macromolecules* **2002**, *35*, 7110.
(3) Qui, X. H.; Moe, N. E.; Ediger, M. D.; Fetters, L. J. *J. Chem. Phys.* **2000**, *113*, 2918.
(4) Schaefer, D.; Spiess, H. W.; Suter, U. W.; Fleming, W. W. *Macromolecules* **1990**, *23*, 3431.
(5) Dekmezian, A.; Axelson, D. E.; Dechter, J. J.; Borah, B.; Mandelkern, L. *J. Polym. Sci., Polym. Phys. Ed.* **1985**, *23*, 367.
(6) Moe, N. E.; Qiu, X. H.; Ediger, M. D. *Macromolecules* **2000**, *33*, 2145.
(7) Lippow, S. M.; Qiu, X. H.; Ediger, M. D. *J. Chem. Phys.* **2001**, *115*, 4961.
(8) Arrighi, V.; Batt-Coutrot, D.; Zhang, C.; Telling, M. T. F.; Triolo, A. *J. Chem. Phys.* **2003**, *119*, 1271.
(9) Fytas, G.; Ngai, K. L. *Macromolecules* **1988**, *21*, 804.
(10) Mieras, H. J. M.; Van Rijn, C. F. H. *J. Appl. Polym. Sci.* **1969**, *13*, 309.
(11) Petraglia, G.; Coen, A. *Polym. Eng. Sci.* **1997**, *10*, 79.
(12) Vinagradov, G.; Prozorovskaya, N. V. *Rheol. Acta* **1964**, *3*, 156.
(13) Fujiyama, M.; Awaya, H. *J. Appl. Polym. Sci.* **1972**, *16*, 275.
(14) Zeichner, G. R.; Patal, P. D. Paper presented at 2nd World Conference on Chemical Engineering, Montreal, Canada, Oct 4−9, 1981.
(15) Plazek, D. L.; Plazek, D. J. *Macromolecules* **1983**, *16*, 1469.
(16) Pearson, D. S.; Fetters, L. J.; Younghouse, L. B.; Mays, J. W. *Macromolecules* **1988**, *21*, 478.
(17) Eckstein, A.; Suhm, J.; Friedrich, C.; Maier, R.-D.; Sassmannshausen, J.; Bochmann, M.; Mulhaupt, R. *Macromolecules* **1998**, *31*, 1335.
(18) Eckstein, A.; Friedrich, C.; Lobbrecht, A.; Spitz, R.; Mulhaupt, R. *Acta Polym.* **1997**, *48*, 41.
(19) Fujiyama, M.; Inata, H. *J. Appl. Polym. Sci.* **2002**, *84*, 2157.
(20) Mavridis, H.; Shroff, R. N. *Polym. Eng. Sci.* **1992**, *32*, 1778.
(21) Londono, J. D.; Maranas, J. K.; Mondello, M.; Habenschuss, A.; Grest, G. S.; Debenedetti, P. G.; Graessley, W. W.; Kumar, S. K. *J. Polym. Sci., Polym. Phys.* **1998**, *36*, 3001.
(22) Schaefer, D.; Spiess, H. W. *J. Chem. Phys.* **1992**, *97*, 7944.
(23) Destree, M.; Laupretre, F.; Lyulin, A.; Ryckaert, J.-P. *J. Chem. Phys.* **2000**, *112*, 9632.
(24) Antoniadis, S. J.; Samara, C. T.; Theodorous, D. N. *Macromolecules* **1998**, *31*, 7944.
(25) Antoniadis, S. J.; Samara, C. T.; Theodorous, D. N. *Macromolecules* **1999**, *32*, 8635.
(26) Destree, M.; Laupretre, F.; Lyulin, A.; Ryckaert, J.-P. *J. Chem. Phys.* **2000**, *112*, 9632.
(27) Gabrys, B.; Higgins, J. S.; Ma, K. T.; Roots, I. *Macromolecules* **1984**, *17*, 560.
(28) Arrighi, V.; Ferguson, R.; Lechner, R. E.; Telling, M. T. F.; Triolo, A. *Physica B* **2001**, *301*, 35.
(29) Arrighi, V.; Gagliardi, S.; Zhang, C.; Ganazzoli, F.; Higgins, J. S.; Ocone, R.; Telling, M. T. F. *Macromolecules* **2003**, *36*, 8738.
(30) Alvarez, F.; Arbe, A.; Colmenero, J. *J. Chem. Phys.* **2000**, *261*, 47.
(31) Farina, M.; Peraldo, M. *Gazz. Chim. Ital.* **1960**, *90*, 973.
(32) Natta, G.; Lombardi, E.; Segre, A. L.; Zambelli, A; Marinangeli, A. *Chim. Ind.* **1965**, *47*, 378.
(33) Zambelli, A.; Segre, A. L.; Farina, M.; Natta, G. *Makromol. Chem.* **1967**, *110*, 1.
(34) Lombardi, E.; Segre, A. L.; Zambelli, A.; Marinangeli, A.; Natta, G. *J. Polym. Sci.* **1967**, *16*, 2539.
(35) Carlile, C. J.; Adams, M. A. *Physica B* **1992**, *182*, 431.
(36) MODES Manual, Rutherford Appleton Laboratory, ISIS, UK.
(37) Howells, W. S. A Fast Fourier Transform Program for the Deconvolution of IN10 Data, RL-81-039, Rutherford Appleton Laboratory, 1981.
(38) Higgins, S.; Benoit, H. C. *Polymers and Neutron Scattering*; Oxford University Press: Oxford, 1993.
(39) Colmenero, J.; Alvarez, F.; Arbe, A. *Phys. Rev. E* **2002**, *65*, 041804.
(40) Zorn, R.; Arbe, A.; Colmenero, J.; Frick, B.; Richter, D.; Buchenau, U. *Phys. Rev. E* **1995**, *52*, 781.
(41) Higgins, J. S.; Allen, G.; Brier, P. N. *Polymer* **1972**, *13*, 157.
(42) Takeuchi, H.; Higgins, J. S.; Hill, A.; Maconnachie, A.; Allen, G.; Stirling, G. C. *Polymer* **1982**, *23*, 499.

MA071412W